

Article

# SVD-Based Image Watermarking Using the Fast Walsh-Hadamard Transform, Key Mapping, and Coefficient Ordering for Ownership Protection

Tahmina Khanam <sup>1</sup>, Pranab Kumar Dhar <sup>1</sup>, Saki Kowsar <sup>1</sup> and Jong-Myon Kim <sup>2,\*</sup> 

<sup>1</sup> Department of Computer Science and Engineering, Chittagong University of Engineering and Technology (CUET), Chattogram-4349, Bangladesh; tahminacse0904079@gmail.com (T.K.); pranabdhar81@gmail.com (P.K.D.); sakikowsar@cuet.ac.bd (S.K.)

<sup>2</sup> School of IT Convergence, University of Ulsan, Ulsan 44610, Korea

\* Correspondence: jmkim07@ulsan.ac.kr; Tel.: +82-52259-2217

Received: 27 October 2019; Accepted: 24 December 2019; Published: 26 December 2019



**Abstract:** Proof of ownership on multimedia data exposes users to significant threats due to a myriad of transmission channel attacks over distributed computing infrastructures. In order to address this problem, in this paper, an efficient blind symmetric image watermarking method using singular value decomposition (SVD) and the fast Walsh-Hadamard transform (FWHT) is proposed for ownership protection. Initially, Gaussian mapping is used to scramble the watermark image and secure the system against unauthorized detection. Then, FWHT with coefficient ordering is applied to the cover image. To make the embedding process robust and secure against severe attacks, two unique keys are generated from the singular values of the FWHT blocks of the cover image, which are kept by the owner only. Finally, the generated keys are used to extract the watermark and verify the ownership. The simulation result demonstrates that our proposed scheme is highly robust against numerous attacks. Furthermore, comparative analysis corroborates its superiority among other state-of-the-art methods. The NC of the proposed method is numerically one, and the PSNR resides from 49.78 to 52.64. In contrast, the NC of the state-of-the-art methods varies from 0.7991 to 0.9999, while the PSNR exists in the range between 39.4428 and 54.2599.

**Keywords:** fast Walsh–Hadamard transform; Gaussian mapping; singular value decomposition; coefficient ordering; key mapping

## 1. Introduction

The flow of multimedia data increases manifold with the recent infrastructural development of computer networks. Accordingly, the proof of ownership issue for multimedia data has come to the surface as an impending challenge. In a bid to negotiate with this problem, the watermarking approach might be used as an indispensable tool. Since multimedia data often suffer from different types of transmission channel attacks, the technique should be immune to such maladies. Hence, the watermarking approach is used for hiding the digital information during transmission. The watermark is typically used to prove the ownership of such host signals. Several algorithms have been proposed in the literature to create robust and imperceptible watermarks. In general, watermarking methods can be divided into three main categories: (i) blind methods [1–13], (ii) semi-blind methods [14–17] (iii) non-blind methods [18–24]. A blind watermarking framework for high dynamic range images (HDRIs) is proposed in [1]. In this method, the artificial bee colony algorithm is employed to select the best block for the embedding watermark. Then, the watermark is inserted in the first level approximation sub-band of the discrete wavelet transform (DWT) of each selected block. This method provides

good quality watermarked images, although it is not robust against geometric attacks such as rotation and scaling. In [2], a new blind error diffusion-based halftone visual watermarking method called content aware double-sided embedding error diffusion (CaDEED) is introduced. By adopting the problem formulation of CaDEED, the optimization problem is solved in order to achieve an optimal solution. Although it shows good results for imperceptibility and robustness, the performance of this system is highly dependent on the content of the host image and watermark. A blind integer wavelet-based watermarking scheme for inserting the compressed version of the binary watermark is presented in [3]. The peak signal-to-noise ratio (PSNR) result of this method is quite satisfactory. However, the robustness against compression attacks is not significant. The authors in [4] proposed a blind geometrically invariant image watermarking method by employing connected objects and a gravity center. This framework has proven resistant against geometrical attacks, such as rotation and scaling. However, it has low robustness against other regular noise attacks such as Gaussian or speckle noise. Furthermore, a contrast-adaptive strategy as a removal solution for visible watermarks is presented in [5] where a sub-sampling technique is adopted to propose such a blind system. The imperceptibility results of this method are very good. However, it shows low robustness against some attacks. In addition to this, a blind watermarking scheme based on singular value decomposition (SVD) is introduced in [6]. Initially, they analyzed the orthogonal matrix  $U$  via SVD. This work utilizes the concept of finding a strong similarity correlation existing between the second-row first column element and the third-row first column element. At the final stage, the color watermark is embedded by slightly modifying the value of the second-row first column element and the third-row first column element of the  $U$  matrix. The technique performs well against various attacks, although it demonstrates very poor performance under median filtering of the watermarked image. Furthermore, the authors in [7] proposed a robust watermarking scheme using discrete cosine transform (DCT) and SVD for lossless copyright protection. Its imperceptibility result is significantly good. However, its robustness result against cropping attacks is quite low. A blind simple watermarking algorithm for image authentication is presented using fractional wavelet packet transform (FRWPT) and SVD in [8]. The proposed algorithm performs the embedding operation on singular values of the host image. To improve the fidelity, the perceptual quality of the watermarked images is exhibited. Although this method is highly secured, it shows low robustness against various attacks for some watermarked images. For estimation of the original coefficients, a blind watermarking method is placed in [9]; the authors used a trained SVR there. Additionally, the particle swarm optimization (PSO) is further utilized to optimize the proposed scheme. It provides high imperceptibility; however, it could not show excellent robustness against several attacks. A blind self-synchronized watermarking method in the cepstrum domain is suggested in [10]. This method does not provide a good trade-off between imperceptibility and robustness. Furthermore, a blind scheme is proposed in [11] in a bid to obtain minimal image distortion. This method provides high-quality watermarked images, albeit low robustness against various attacks. In [12], hamming codes are used to embed the authentication information in a cover image. The watermark extraction process of this method is blind and provides satisfactory results in imperceptibility. However, the robustness result against various attacks is not reported there. The authors of [13] suggested a blind watermarking algorithm based on lower-upper (LU) decomposition. The watermark is embedded into the first-column second-row element and the first-column third-row element of the lower triangular matrix obtained from LU decomposition. It provides good quality watermarked images despite the low robustness against compression attacks. A semi-blind self-reference image watermarking method using discrete cosine transform (DCT) and singular value decomposition (SVD) is proposed in [14]. Initially, essential blocks are fetched by using a threshold on the number of edges in each block. Using these essential blocks, a reference image is created and then transformed into the DCT and SVD domain. Embedding the watermark is done by modifying singular values of the host image using singular values of the watermark image. This method yields good quality watermarked images. However, it shows low robustness against the scaling operation. To embed the watermark, the concepts of vector quantization (VQ) and association

rules in data mining are employed in [15]. The approach is semi-blind, which hides the association rules of the watermark instead of the whole watermark. This method shows good robustness against various attacks with poor performance on imperceptibility. In addition, a reference watermarking scheme with semi-blind is proposed in [16] based on DWT and SVD for copyright protection and authenticity. The method has high imperceptibility showing the low robustness against cropping and rotation attacks. An image watermarking method using DWT, all phase discrete cosine bi-orthogonal transform (APDCBT), and SVD is proposed in [17]. This method shows high imperceptibility; however, it provides low robustness against combined cropping and compression attacks. A non-blind image watermarking algorithm based on the Hadamard transform is proposed in [18]. In this method, the breadth first search (BFS) technique is used to embed the watermark. Notably, it shows good performance in imperceptibility. However, it has the limitation of relatively poor performance against compression attacks. The authors in [19] introduced a non-blind robust watermarking technique using DCT and a normalization procedure. They used image normalization for calculating the affine transform parameters so that the watermark embedding and detection processes can be performed in the original coordinate system. However, this method shows low robustness against some attacks. In [20], a non-blind digital watermarking algorithm using wavelet-based contourlet transform (WBCT) is presented. To select the position for inserting the watermark, the texture information of the image is used. It has good robustness against numerous attacks, albeit low robustness against filtering attacks. Moreover, the imperceptibility result of this method is not reported there. A non-blind hybrid image watermarking scheme based on DWT and SVD is proposed in [21]. In this approach, the watermark is embedded to the elements of singular values of the cover image of DWT sub-bands. The imperceptibility result of this method is quite high, having low the robustness against cropping attacks. A non-blind SVD-based digital watermarking scheme for ownership protection is proposed in [22]. In this method, a meaningful text message is used rather than using a randomly generated Gaussian sequence. However, the robustness of this method against attacks is low. A non-blind image watermarking using DCT and DWT is proposed in [23]. The DCT coefficients of the watermark image are embedded into four DWT bands of the color components of the host image. The imperceptibility result of this method is quite satisfactory. However, the robustness against rotation attacks is a little low. A non-blind color image watermarking method using SVD and QR code is suggested in [24]. This method shows good results in imperceptibility; the robustness result against poison and speckle noise attack is not reported.

From the above studies, we can conclude that some methods have low robustness, whereas some methods have less imperceptible or less secured. Further, some methods are non-blind and semi-blind. To overcome these limitations, an SVD-based blind symmetric image watermarking method using fast Walsh–Hadamard transform (FWHT) with key mapping and coefficient ordering for ownership protection is proposed in this paper. In symmetric watermarking, the same keys are used for embedding and detecting the watermark. The major contributions of this research work are subjected:

- A blind image watermarking method is proposed that is highly robust and secured against numerous attacks while providing good quality watermarked images;
- To safeguard the unauthorized detection, the Gaussian mapping is used to scramble the watermark;
- To facilitate authentic and errorless extraction of the watermark image by generating the keys from the singular values the FWHT blocks of the cover image;
- It provides a good trade-off among robustness, security, and imperceptibility.

Simulation results indicated that our proposed method is highly robust against numerous attacks. The normalized correlation (NC) of the proposed method is numerically one, whereas the NC of the recent methods [13,23,24] vary from 0.7991 to 0.9999. The peak signal-to-noise ratio (PSNR) of the proposed method varies from 49.78 to 52.64, whereas the PSNR of the recent methods [13,23,24] vary from 39.4428 to 54.2599. In other words, the proposed method outperforms state-of-the-art methods in terms of robustness, security, and imperceptibility.

The rest of the paper is organized as follows. Section 2 introduces the background information, whereas the proposed watermarking method is illustrated in Section 3. Section 4 provides the experimental results. Finally, the paper is concluded in Section 5 with future remarks.

## 2. Background Information

### 2.1. Singular Value Decomposition

For an  $M \times M$  square matrix  $X$  with  $\text{rank} \leq M$ , its SVD is represented by Equation (1):

$$X = UDV^T$$

$$X = \begin{bmatrix} U_{1,1} & \cdots & U_{1,M} \\ U_{2,1} & \cdots & U_{2,M} \\ \vdots & \ddots & \vdots \\ U_{M,1} & \cdots & U_{M,M} \end{bmatrix} \begin{bmatrix} \lambda_1 & 0 & \cdots & 0 \\ 0 & \lambda_2 & \cdots & 0 \\ \vdots & \vdots & \ddots & \vdots \\ 0 & 0 & \cdots & \lambda_M \end{bmatrix} \begin{bmatrix} v_{1,1} & \cdots & v_{1,M} \\ v_{2,1} & \cdots & v_{2,M} \\ \vdots & \ddots & \vdots \\ v_{M,1} & \cdots & v_{M,M} \end{bmatrix} \quad (1)$$

where  $U$  and  $V$  are  $M \times M$  orthogonal matrices, and  $D$  is a singular diagonal matrix with diagonal elements  $\lambda_1, \lambda_2, \lambda_3, \dots, \lambda_M$ . These diagonal elements are unique for image data. Therefore, these values are used to generate unique keys for the errorless and authentic extraction of the watermarks.

### 2.2. Fast Walsh-Hadamard Transform

General Hadamard transform is performed by a Hadamard matrix  $H$  with the size  $4 \times 4$  defined in Equation (2). It is an orthogonal square matrix with only +1 and -1 values. Furthermore, it has a unique sequence that is counted on the basis of the changes of the values in a row.

$$H = \begin{bmatrix} 1 & 1 & 1 & 1 \\ 1 & -1 & 1 & -1 \\ 1 & 1 & -1 & -1 \\ 1 & -1 & -1 & 1 \end{bmatrix} \quad (2)$$

The Hadamard transform concentrates most of the energy into the upper left corner of the transformed matrix. The direct current (DC) and alternating current (AC) coefficients of the transform matrix are arranged in zigzag order from low-frequency components to high-frequency components. In this study, the low-frequency components are used for embedding the watermark, since they are less sensitive to noise. Additionally, the Hadamard matrix has a different form called Walsh matrix  $W$ , which is defined in Equation (3).

$$W = \begin{bmatrix} 1 & 1 & 1 & 1 \\ 1 & 1 & -1 & -1 \\ 1 & -1 & -1 & 1 \\ 1 & -1 & 1 & -1 \end{bmatrix} \quad (3)$$

In this proposed method, fast Walsh-Hadamard transform (FWHT) is utilized, which is a technique of calculating a discrete Walsh-Hadamard transform with less computation time.

## 3. Proposed Method

Let  $X = \{x(i, j), 1 \leq i \leq M, 1 \leq j \leq M\}$  be the original host image and  $W = \{w(k, l), 1 \leq k \leq N, 1 \leq l \leq N\}$  be the watermark image to be embedded into the original image.

### 3.1. Watermark Preprocessing

It is essential to preprocess the watermark for enhancing its security. Preprocessing includes the scrambling of the watermark image. In this proposed method, we utilize Gaussian mapping to scramble the watermark. To implement the Gaussian mapping on the watermark, the following steps are performed:

- Step 1.** The watermark image  $W$  is reshaped into a one-dimensional sequence  $Q = \{q(r), 1 \leq r \leq N \times N\}$ .
- Step 2.** Initially, a reference pattern  $P = \{p(r), 1 \leq r \leq N \times N\}$  is generated using a Gaussian map, which is defined in Equation (4).

$$p(r) = \exp\{-a \times (p(r+1))^2\} + b \quad (4)$$

where  $a$ ,  $b$ , and  $p(1)$  are predefined constants and are used as key  $k3$ , as shown in Figure 1.

- Step 3.** Then, the binary reference pattern  $Z = \{z(r), 1 \leq r \leq N \times N\}$  is calculated using the following equation:

$$z(r) = \begin{cases} 1 & \text{if } p(r) > T \\ 0 & \text{otherwise} \end{cases} \quad (5)$$

where  $T$  is a predefined threshold.

- Step 4.** Finally, the watermark sequence  $q(r)$  is scrambled with  $z(r)$  using Equation (6):

$$u(r) = z(r) \oplus q(r), \quad 1 \leq r \leq N \times N \quad (6)$$

where  $\oplus$  denotes the bitwise XOR operation.

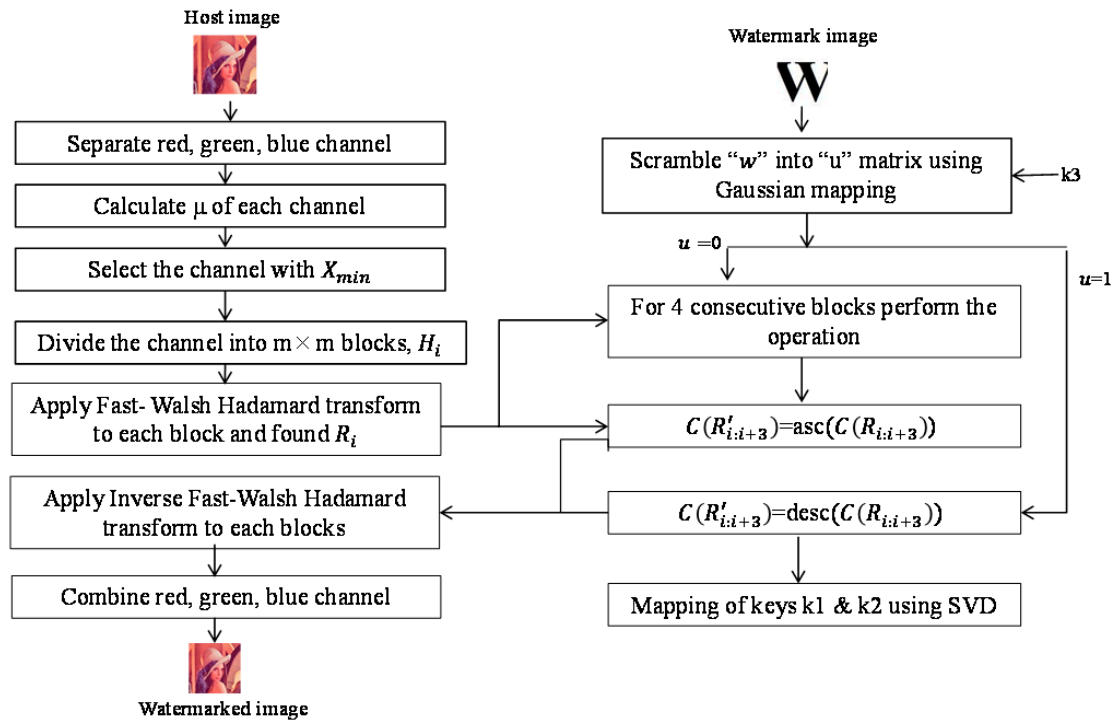


**Figure 1.** Proposed embedding algorithm.

### 3.2. Watermark Embedding Process

The proposed watermark embedding process is shown in Figure 1. The pseudo code of the watermark embedding process is presented in Algorithm 1. The embedding process is described in the following steps:

- Step 1.** The original host image  $X$  is first divided into three channels  $X_{red}$ ,  $X_{green}$ , and  $X_{blue}$ , where  $X_{red}$ ,  $X_{green}$ , and  $X_{blue}$  represent the red, green, and blue channels of the original image, respectively. Then, the mean of the pixel values of each channel is calculated using Equation (7).

$$\mu(X_{red}) = \sum_{i=1}^M \sum_{j=1}^M \frac{X_{red}}{255}, \mu(X_{green}) = \sum_{i=1}^M \sum_{j=1}^M \frac{X_{green}}{255}, \mu(X_{blue}) = \sum_{i=1}^M \sum_{j=1}^M \frac{X_{blue}}{255} \quad (7)$$

where  $\mu(X_{red})$ ,  $\mu(X_{green})$ , and  $\mu(X_{blue})$ , indicate the mean of the pixel values of the red, green, and blue channels, respectively. After that, the channel with minimum mean  $X_{min}$  is selected, which is either  $X_{red}$ ,  $X_{green}$ , or  $X_{blue}$ .

- Step 2.** The selected channel  $X_{min}$  is further divided into  $m \times m$  non-overlapping blocks,  $H = \{H_i; 1 \leq i \leq n\}$ , where  $i$  is the block number and  $m$  is the length of the row and column of each block.
- Step 3.** FWHT is applied in each block  $H_i$  to obtain the transformed block  $R_i$ , where  $R_i$  contains the FWHT coefficients.
- Step 4.** Among all the  $n$  blocks, each set of four consecutive blocks  $R_i, R_{i+1}, R_{i+2}$ , and  $R_{i+3}$  is selected to embed a watermark bit. The main idea of the embedding process is to sort the coefficients of the first row represented by  $C(R_{i:i+3})$ , where  $\{i : i + 3\}$  indicates  $\{i, i + 1, i + 2, i + 3\}$  of each set of selected blocks  $R_i, R_{i+1}, R_{i+2}$ , and  $R_{i+3}$  except the DC value. If the watermark bit is 1, the selected low-frequency coefficients  $C(R_{i:i+3})$  are sorted in descending order; otherwise, they are sorted in ascending order. The concept of embedding the watermark bit in ascending and descending order with a block size of  $4 \times 4$  where,  $m = 4$ , is shown in Figure 2.

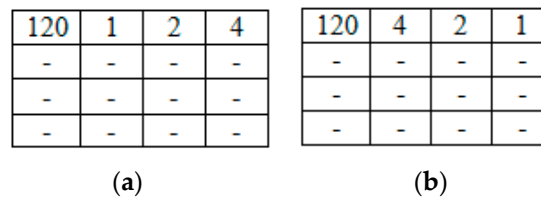


**Figure 2.** (a) Sorting in ascending order to embed 0 bits and (b) sorting in descending order to embed 1 bit.

In this step, two keys  $k1$  and  $k2$  are also used in order to make the watermarking method more secured. The key  $k1$  is generated from the singular values of each block  $H_i$  of the selected channel of host image. The key  $k2$  is generated from key  $k1$ , which is used to authenticate key  $k1$  in the watermark extraction process. The following operation is performed for embedding a watermark bit into each selected block.

$$\begin{aligned} C(R'_{i:i+3}) &= asc(C(R_{i:i+3})); \text{ mapping key } k1 \text{ and } k2, \quad \text{when } u(r) = 0 \\ C(R'_{i:i+3}) &= desc(C(R_{i:i+3})); \text{ mapping key } k1 \text{ and } k2, \quad \text{when } u(r) = 1 \end{aligned} \quad (8)$$

where  $asc$  and  $desc$  represent sorting the data in ascending order and descending order, respectively. The process of mapping the keys  $k1$  and  $k2$  are described in the next section.

**Mapping key  $k1$  and  $k2$ :** In this section, the process of mapping keys  $k1$  and  $k2$  is explained, which is defined in Equation (8). This step is introduced to strengthen the proposed algorithm under severe attack. To map the keys initially, SVD is applied in each block  $H_i$  to generate the necessary information. To perform the operation, the following steps are used:

- (1) Each block  $H_i$  of the selected channel is decomposed into three matrices:  $U_i, D_i$ , and  $V_i$  using Equation (9).

$$H_i = U_i D_i V_i^T \quad (9)$$

where  $\lambda_{i1}, \lambda_{i2}, \dots, \lambda_{im}$  are the singular values of the matrix  $D_i$  of each block  $H_i$ . These singular values are unique for each block  $H_i$ . The keys  $k1$  and  $k2$  are calculated using these

singular values. Thus, unauthorized people could not map the keys without the host image to prove fake ownership. To do this, initially, a null key  $k1$  is defined. Then,  $k1$  is generated using these singular values as defined in Equation (10) below:

$$k1 = \text{append}(k1, (\text{asc}(\lambda_{ij}))), u(r) = 0 \quad k1 = \text{append}(k1, (\text{desc}(\lambda_{ij}))), u(r) = 1 \quad (10)$$

where  $i$  indicates the block number,  $j = \{1 \leq j \leq m\}$  indicates the singular values of each block,  $\text{asc}$  and  $\text{desc}$  represent sorting the data in ascending order and descending order, respectively, and  $\text{append}$  indicates the concatenation operation. The singular values are sorted according to the watermark bit 0 or 1.

- (2) Finally,  $k1$  is converted into a one-dimensional sequence of length  $L = n \times m$ , where  $n$  is the total number of blocks and  $m$  is the total number of singular values in each block.
- (3) To generate key  $k2$ , define a null key  $k2$  with length  $S$ , where  $S = n/m$ . Then,  $k2$  is generated from key  $k1$  using the following Equation (11):

$$k2 = \text{append}(k2, \mu(k1_{n:h+t})) \text{ where } 1 \leq h \leq L \quad (11)$$

where  $\mu$  is the mean of consecutive  $t$  values of key  $k1$  and the length of key  $k2$  is  $(n/m) + 1$ . Although the first key can be generated by the owner only, the second key is generated to authenticate the first key in the extraction process.

**Step 5.** Inverse FWHT is applied to each transformed block  $R'_i$  and the watermarked blocks  $H'_i$  are found.

**Step 6.** Finally, three watermarked channels  $X'_{red}$ ,  $X'_{green}$ , and  $X'_{blue}$  are combined to generate the watermarked image  $X'$ .

---

#### Algorithm 1: Watermark Insertion

---

Variable Declaration:

$X$ : Host image

$\mu$ : Mean intensity value of each channel of host image (Lena)

$X_{min}$ : Channel with minimum mean

$H_i$ : Non-overlapping blocks of  $X_{min}$  (size  $4 \times 4$ )

FWHT, SVD: Transformation and decomposition used in the algorithm

$R_i$ : FWHT transformed block of  $H_i$

$C(R_{i:i+3})$ : Three coefficients of first row (except DC value) of the consecutive transformed block

$C(R'_{i:i+3})$ : Coefficients in ascending or descending order

$W$ : Watermark image

$u$ : Scrambled watermark sequence

Watermark Embedding Procedure:

1. Watermark preprocess: scramble  $W$  to obtain  $u$  using Gaussian mapping

2. Read the host image and calculate  $\mu$  of each channel (Red, Green, Blue)

$X.bmp$  (host image with size of  $256 \times 256$ )

$W.bmp$  (watermark image with size of  $32 \times 32$ )

3. Select channel  $X_{min}$  and divide it into  $4 \times 4$   $H_i$  blocks

4. Apply FWHT to each block  $H_i$  and found  $R_i$

5. Watermark Insertion

$$C(R'_{i:i+3}) = \text{asc}(C(R_{i:i+3})); \text{ mapping key } k1 \text{ and } k2, \text{ when } u(r) = 0$$

$$C(R'_{i:i+3}) = \text{desc}(C(R_{i:i+3})); \text{ mapping key } k1 \text{ and } k2, \text{ when } u(r) = 1$$

$\text{asc}$ : ascending order,  $\text{desc}$ : descending order,  $1 \leq r \leq 32 \times 32$

// Use SVD to map keys  $k1$  and  $k2$

6. Perform inverse FWHT and combine the channels to get the Watermarked Image

---

### 3.3. Watermark Detection Process

The watermark extraction process has two main phases: (1) modify the degree of ascendant/descendant of the attacked watermarked image with key  $k_1$ , and (2) authenticate key  $k_1$  with key  $k_2$ . In addition, the pseudo code of the watermark detection process is presented in Algorithm 2. The overall process is described below and shown in Figure 3:

- Step 1.** The attacked watermarked image  $X^*$  is first divided into three channels,  $\{X_{red}^*, X_{green}^*, \text{ and } X_{blue}^*\}$ . Then, the mean value of the pixels of the red, green, and blue channels represented by  $\mu(X_{red}^*)$ ,  $\mu(X_{green}^*)$ , and  $\mu(X_{blue}^*)$  are calculated. Thereafter that, the channel with minimum mean  $X_{min}^*$  is selected for extracting the watermark.
- Step 2.** The selected channel  $X_{min}^*$  is further divided into  $m \times m$  non-overlapping blocks  $H_i^*$ , where  $i$  is the block number.
- Step 3.** FWHT is carried out on each block  $H_i^*$ . After applying this operation, the transformed blocks  $R_i^*$  are found.
- Step 4.** The degree of ascendant/descendant denoted by  $dof$  is calculated for four consecutive transformed blocks  $\{R_i^*, R_{i+1}^*, R_{i+2}^*, R_{i+3}^*\}$ . Therefore,  $dof(asc)$  represents the number of times that the low-frequency coefficients in the first row  $C^*(R_{i:i+3}^*)$  of each transformed block except for the DC value are in ascending order. Similarly, the  $dof(desc)$  represents the number of times that the low-frequency coefficients in the first row  $C^*(R_{i:i+3}^*)$  of each transformed block except the DC value are in descending order.

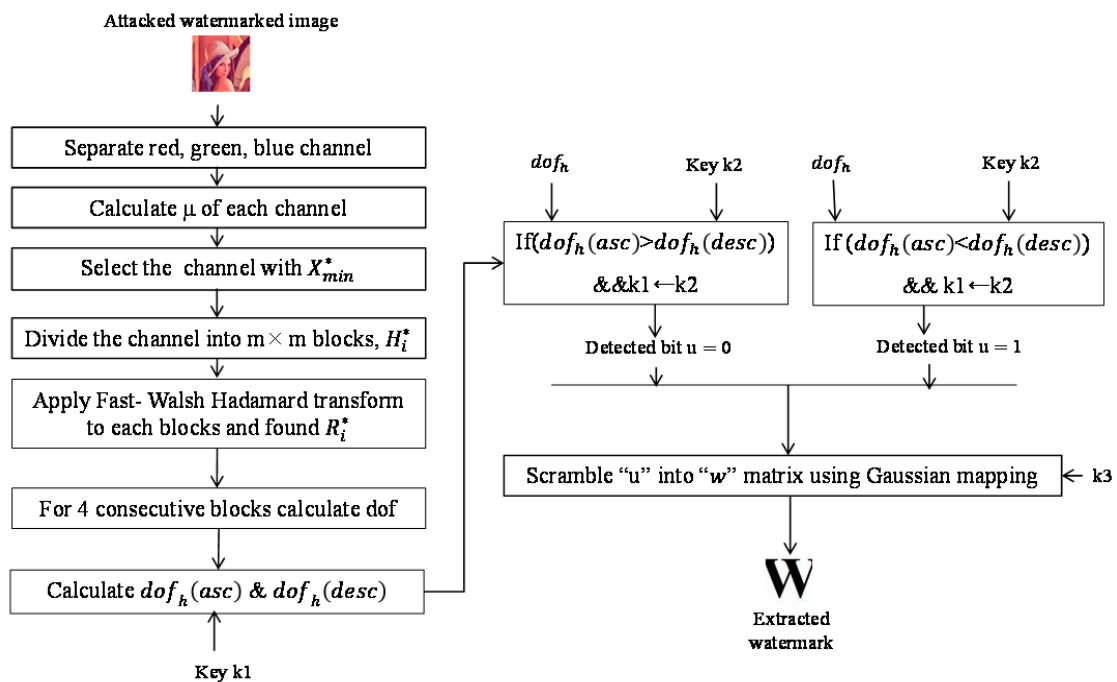


Figure 3. Proposed extraction algorithm.

Later,  $dof$  is modified with key  $k_1$ . This phase assists the system to resist when the noise attack is severe. Initially, the  $dof'$  of the first  $t$  values of key  $k_1$  is calculated to extract the first watermark bit using Equations (12) and (13). Thus, consecutive  $t$  values of the key are considered each time for extracting a one-bit watermark. We found another two matrices,  $dof'(asc)$  and  $dof'(desc)$ , with  $\frac{L}{t} = N^2$  values, where  $L$  is the length of key  $k_1$ , with  $1 \leq h \leq L$ .

$$dof'(asc) = dof'(asc) + 1; \text{ if } k1_h > k1_{h+1} \tag{12}$$

$$dof'(desc) = dof'(desc) + 1; fk1_h < k1_{h+1} \quad (13)$$

Finally, we modify the  $dof$  with  $dof'$  by a simple addition operation, as shown in Equations (14) and (15), and found two matrices,  $dof_h(asc)$  and  $dof_h(desc)$ .

$$dof_h(asc) = dof(asc) + dof'(asc) \quad (14)$$

$$dof_h(desc) = dof(desc) + dof'(desc) \quad (15)$$

**Authenticate  $k1$  with  $k2$ :** This operation is carried out to authenticate key  $k1$  using  $k2$ . For this purpose, the average of the consecutive  $t$  values of  $k1$  is calculated and compared with one value of  $k2$ . This operation is represented using Equations (16) and (17) given below:

$$if(\mu(k1_{h:h+t})) = k2_h; k1 \leftarrow k2 \quad (16)$$

$$if(\mu(k1_{h:h+t}))! = k2_h; !k1 \leftarrow k2 \quad (17)$$

where  $k1 \leftarrow k2$  means  $k1$  is authenticated by  $k2$  and  $!k1 \leftarrow k2$  means  $k1$  is not authenticated by  $k2$ . If  $k1$  is authenticated, then the watermark would be extracted accordingly.

**Step 5.** The hidden binary sequence is found using the following rule:

---

**If**  $dof_h(asc) > dof_h(desc)$  and  $k1 \leftarrow k2$   
 then  $u(r) = 0$   
**else If**  $dof_h(asc) > dof_h(desc)$  and  $k1 \leftarrow k2$   
 then  $u(r) = 1$

---

**Step 6.** The binary watermark sequence  $q^*(r)$  is extracted with key  $k3$  using the following equation:

$$q^*(r) = z(r) \oplus u(r), \quad 1 \leq r \leq N \times N. \quad (18)$$

Finally, the watermark image  $W^*$  is found by arranging the watermark sequence  $q^*(r)$  into the  $N \times N$  matrix.

---

#### Algorithm 2: Watermark Extraction

---

Variable Declaration:

$X^*$ : Attacked watermarked image

$\mu$ : Mean intensity value of each channel of  $X^*$

$X_{min}^*$ : Channel with minimum mean

$H_i^*$ : Non-overlapping blocks of  $X_{min}^*$  (size  $4 \times 4$ )

FWHT: Transformations used in the algorithm

$R_i^*$ : FWHT transformed block of  $H_i^*$

$C^*(R_{i:i+3}^*)$ : Three coefficients of first row (except DC value) of four consecutive transformed block

$W$ : Watermark image

$u$ : Scrambled watermark sequence

$dof(asc/desc)$ : The number of times low-frequency coefficients in the first row  $C^*(R_{i:i+3}^*)$  of each transformed block except the DC value are in ascending/descending order.

Watermark Extraction Procedure:

1. Read  $X^*$  and calculate  $\mu$  of each channel (Red, Green, Blue)
  2. Select channel  $X_{min}^*$  and divide into  $4 \times 4$   $H_i^*$  blocks
  3. Apply FWHT to each block  $H_i^*$  and found  $R_i^*$
  4. Watermark extraction
-

---

(a) Modifying  $dof(asc/desc)$  into  $dof'(asc/desc)$  with key  $k1$

$$dof'(asc) = dof(asc) + 1; \text{ if } k1_h > k1_{h+1}$$

$$dof'(desc) = dof(desc) + 1; \text{ if } k1_h < k1_{h+1}$$

where  $L$  is the length of key  $k1$ , with  $1 \leq h \leq L$  and then calculate

$$dof_h(asc) = dof(asc) + dof'(asc)$$

$$dof_h(desc) = dof(desc) + dof'(desc)$$

(b) Authenticate key  $k1$  with key  $k2$

$$\text{if}(\mu(k1_{h:h+t})) = k2_h; k1 \leftarrow k2$$

$$\text{if}(\mu(k1_{h:h+t})) \neq k2_h; !k1 \leftarrow k2$$

where  $k1 \leftarrow k2$  means  $k1$  is authenticated by  $k2$  and  $!k1 \leftarrow k2$  means  $k1$  is not authenticated by  $k2$ .

// Consecutive  $t$  values of the key are considered each time for extracting a one-bit watermark, where  $\frac{L}{t} = N^2$  and  $\mu(k1_{h:h+t})$  means mean of these  $t$  values

(c) Watermark extraction

If  $dof_h(asc) > dof_h(desc)$  and  $k1 \leftarrow k2$

then  $u(r) = 0$

else If  $dof_h(asc) < dof_h(desc)$  and  $k1 \leftarrow k2$

then  $u(r) = 1$

where,  $1 \leq r \leq 32 \times 32$

(d) Re-scramble  $u$  to get  $W$

---

#### 4. Experimental Results and Discussions

In this section, the performance of our proposed method is evaluated in terms of imperceptibility and robustness. The proposed method used various images, including Lena, Peppers, Baboon, and Fruit, with the size  $256 \times 256$  as host images shown in Figure 4. The size of the binary watermark image is  $32 \times 32$ , as shown in Figure 5. It performs well for all the host images in term of imperceptibility and robustness. In this study, the selected values for  $m$  and  $t$  are 4 and 16, respectively, as the size of each block  $H_i$  is  $4 \times 4$ . Therefore, the total number blocks is 4096. Thus, the length of the key  $k1$  is 16384. The main reason for selecting a smaller value for  $m$  to embed the watermark bit is that sorting larger blocks causes greater degradation in the quality of the watermarked image.

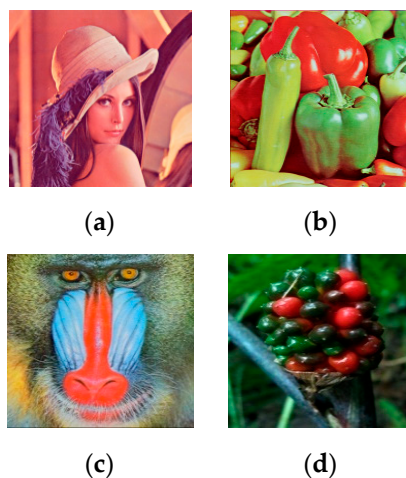


**Figure 4.** The host images: (a) Lena, (b) Peppers, (c) Baboon, and (d) Fruit.

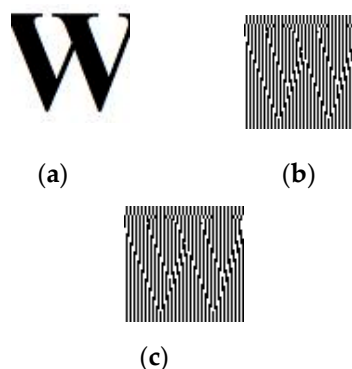


**Figure 5.** Watermark images: (a) original, (b) scrambled with  $a = 10$ ,  $b = 0.05$ , and  $y_0 = 20$ , and (c) scrambled with  $a = 30$ ,  $b = 0.01$ , and  $y_0 = 10$ .

**Imperceptibility test:** The imperceptibility of the watermarked images can be evaluated in terms of the peak signal-to-noise ratio (PSNR), as given in Equation (19).

$$\text{PSNR} = 10 \log_{10} \left( \frac{255^2}{\frac{1}{MM} \sum_{i=1}^M \sum_{j=1}^M (X - X')^2} \right) \quad (19)$$

where  $X$  and  $X'$  are the original and watermarked images, respectively. Higher values of PSNR indicate the better quality of the watermarked image. Figure 4 shows the original and scrambled images with different values of  $a$ ,  $b$ , and  $y_0$ .

To test the imperceptibility of the proposed framework, the PSNR values are calculated and compared with those values of the existing methods, as shown in Table 1. From this table, it is observed that the PSNR of the proposed method varies from 49.78 to 52.64, whereas the PSNR of the recent methods [13,23,24] varies from 47.1961 to 47.1836, 54.2577 to 54.2599, and 39.4428 to 40.8216. Therefore, it is evident that the PSNRs of the recent methods [23,24] are quite high, whereas the PSNRs of the recent method [13] are low compared to all other methods. In other word, the PSNR of the proposed method is higher than that of the methods reported in [13]. However, it is slightly lower than that of the method reported in [24]. This comparison justifies that the suggested method outperforms the other recent techniques. Since in each  $4 \times 4$  block, only three AC values are shuffled, and the DC value remains in its position, low image degradation took place. However, low image degradation results in high imperceptibility.

**Security analysis:** For a secured watermarking method, how it performs against various attacks is very important. The proposed method utilizes a Gaussian map to enhance the security. To encrypt the watermark image, some predefined constants are used such as  $a$ ,  $b$ , and  $p(1)$ , which are considered as secret key  $k_3$ . If the selected value for  $a$ ,  $b$ , and  $p(1)$  are wrong, in that case, the watermark will not be extracted properly. Further, in order to make the watermarking method more secured, the two keys  $k_1$  and  $k_2$  are used. The key  $k_1$  is generated from the singular values of each block  $H_i$  of the selected channel of host image. Moreover, it is observed that these singular values are floating point numbers, and it is not possible to find out these singular values without the host image. Therefore, it is not possible to generate key  $k_1$  without the host image. The key  $k_2$  is generated from key  $k_1$ , which is used to authenticate the key  $k_1$  in the watermark extraction process. Therefore, it is not possible to generate the key  $k_2$  without  $k_1$ . These keys ( $k_1$ ,  $k_2$ ,  $k_3$ ) are used in the watermark detection process to extract the embedded watermark. The correct watermark can be extracted when all the keys ( $k_1$ ,  $k_2$ , and  $k_3$ ) are correct. In other words, if any one of the keys is wrong, then the watermark will not be extracted correctly. This phenomenon is illustrated in Figure 6. Moreover, the size of each block  $H_i$  of the selected channel of the host image is  $4 \times 4$ ; therefore, the total number of blocks in each host image is 4096. Thus, the length of the key  $k_1$  is  $4096 \times 4 = 16,384$ , and the length of the key  $k_2$  is  $(4096/4) + 1 = 1025$ ,

which are quite long, indicating that the key space is large enough. As the key  $k_1$ ,  $k_2$ , and  $k_3$  are floating point numbers, therefore, the value of these keys cannot be determined. Hence, the probability of extracting the right watermark is near to 0. Therefore, the attacker cannot detect the correct watermark without the right key, which enhances the security of the proposed watermarking method.

**Table 1.** Comparison between the proposed and recent methods in terms of peak signal-to-noise ratio (PSNR).

Watermarked Images	Proposed Method	Ahmed et al. [23]	Patvardhar et al. [24]	Su et al. [13]
	50.04		54.2577	39.4428
	49.78	47.1961		40.8216
	51.56	47.1836	54.3499	
	52.64			

Key	Case 1	Case 2	Case 3	Case 4
Key $k_1$	√	×	√	√
Key $k_2$	√	√	×	√
Key $k_3$	√	√	√	×

Extracted watermark    

**Figure 6.** The extracted watermark with right and different wrong keys.

**Robustness test:** To measure the robustness of the proposed algorithm, the normalized correlation (NC) is calculated between the original watermark image and the extracted watermark image. The NC value is calculated using Equation (20):

$$NC(W, W^*) = \frac{\sum_{k=1}^N \sum_{l=1}^N w(k, l) \cdot w^*(k, l)}{\sqrt{\sum_{k=1}^N \sum_{l=1}^N w(k, l) \cdot w(k, l)} \sqrt{\sum_{k=1}^N \sum_{l=1}^N w^*(k, l) \cdot w^*(k, l)}} \quad (20)$$

where  $W$  and  $W^*$  are the original watermark and extracted watermark, respectively.

Now, the main fact is to consider the different types of noise attacks on the watermarked image. The results are illustrated in such a way as to identify the effect of keys on the NC values. Figures 7–9 show the effect of keys in a pictorial way, including the PSNR and NC values.

Attack type		Lena	Peppers	Baboon	Fruit
No attack	Watermarked image				
	PSNR	50.04	49.78	51.56	52.64
	Extracted watermark (with and without keys)				
	NC (with and without keys)	1.0 and 1.0	1.0 and 1.0	1.0 and 1.0	1.0 and 1.0
Gaussian noise (0.1)	Watermarked image				
	Extracted watermark (with and without keys)				
	NC (with and without keys)	1.0 and 0.9997	1.0 and 0.9823	1.0 and 1.0	1.0 and 0.9351
Speckle noise (0.01)	Watermarked image				
	Extracted watermark (with and without keys)				
	NC (with and without keys)	1.0 and 0.8835	1.0 and 0.9292	1.0 and 0.9068	1.0 and 0.9349

Figure 7. Cont.

	Watermarked image				
Salt and pepper noise (0.01)	Extracted watermark (with and without keys)				
	NC (with and without keys)	1.0 and 0.9945	1.0 and 0.9931	1.0 and 0.9956	1.0 and 0.9944

Figure 7. Analysis of proposed method under No attack, Gaussian noise (0.01), Speckle noise, and Salt and Pepper noise (0.01). NC: normalized correlation.

Attack type		Lena	Peppers	Baboon	Fruit
Adjustment	Watermarked image				
	Extracted watermark (with and without keys)				
	NC (with and without keys)	1.0 and 0.9543	1.0 and 0.7544	1.0 and 0.9014	1.0 and 0.6137
Cropped (50%)	Watermarked image				

Figure 8. Cont.

	Extracted watermark (with and without keys)				
	NC (with and without keys)	1.0 and 0.7919	1.0 and 0.7821	1.0 and 0.7912	1.0 and 0.7866
Sharpening (tolerance = 0.1)	Watermarked image				
	Extracted watermark (with and without keys)				
	NC (with and without keys)	1.0 and 0.9578	1.0 and 0.9335	1.0 and 0.9241	1.0 and 0.8594
Weiner filtering	Watermarked image				
	Extracted watermark (with and without keys)				
	NC (with and without keys)	1.0 and 0.6753	1.0 and 0.6785	1.0 and 0.6884	1.0 and 0.6771

**Figure 8.** Analysis of proposed method under Adjustment, Cropping (50%), Sharpening (0.1), and Weiner filtering.

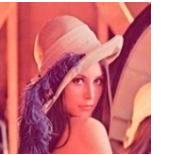
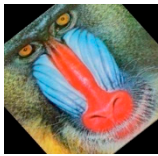
Attack type		Lena	Peppers	Baboon	Fruit
Poison noise	Watermarked image				
	Extracted watermark (with and without keys)				
	NC (with and without keys)	1.0 and 0.9950	1.0 and 0.9963	1.0 and 0.9992	1.0 and 0.9990
Median filtering	Watermarked image				
	Extracted watermark (with and without keys)				
	NC (with and without keys)	1.0 and 0.9762	1.0 and 0.9541	1.0 and 0.9896	1.0 and 0.9459
Compression (quality factor: 50%)	Watermarked image				
	Extracted watermark (with and without keys)				
	NC (with and without keys)	1.0 and 0.5775	1.0 and 0.5936	1.0 and 0.5912	1.0 and 0.5676

Figure 9. Cont.

Rotation (40°)	Watermarked image				
	Extracted watermark (with and without keys)				
	NC (with and without keys)	1.0 and 0.5160	1.0 and 0.5132	1.0 and 0.5194	1.0 and 0.5193

**Figure 9.** Analysis of the proposed method under Poison noise, Median filtering, Compression (quality factor: 50%), and Rotation.

Furthermore, Tables 2 and 3 show an overview of the NC values of the proposed scheme with keys and without keys, respectively. Notably, the NC values shown in Table 2 reflect better results than Table 3. This is because severe noise attacks affect the degree of ascendant/descendant ( $dof$ ). This  $dof$  is derived without key  $k1$  and is vulnerable to noise attack until it is modified with  $dof'$ , as defined in Equations (14) and (15). Since the keys make the system effectively resistant against noise, Table 3 shows better results in terms of NC. Further, the extracted watermarks from four different watermarked images under Gaussian noise with tolerance 0.1 are shown in Figure 7. The extracted watermark using only  $dof$  (without key) for the "Fruit" cover image provides lower NC values than the others. Since the color variation in this host image is not very high,  $dof$  (without keys) is more vulnerable under additive noise attack. This is also applicable for other attacks, such as adjustment and sharpening, as shown in Figure 8. This problem is overcome in the proposed framework with the concept of key mapping. In spite of the high noise attack, extracting the watermark using  $dofk$  (with keys) could reconstruct the watermark image successfully with a unity of NC values, as shown in Figures 7–9. We observed that the NC of the proposed method against various attacks is numerically one. It is because the keys ( $k1$ ,  $k2$  and  $k3$ ) that contain the necessary information of the watermark are not affected by various attacks. Hence, this proposed technique ensures high robustness.

**Table 2.** NC values after applying various noise attacks (with keys).

No	Attack Type	Lena	Peppers	Baboon	Fruit
1	Gaussian (0.01)	1.0	1.0	1.0	1.0
2	Speckle (0.01)	1.0	1.0	1.0	1.0
3	Adjustment	1.0	1.0	1.0	1.0
4	Cropping (50%)	1.0	1.0	1.0	1.0
5	Sharpening (tol = 0.1)	1.0	1.0	1.0	1.0
6	Rotation ( $40^0$ )	1.0	1.0	1.0	1.0
7	Wiener filtering	1.0	1.0	1.0	1.0
8	Poison noise	1.0	1.0	1.0	1.0
9	Salt and pepper noise (0.01)	1.0	1.0	1.0	1.0
10	Median filtering	1.0	1.0	1.0	1.0
11	Compression (quality factor = 50%)	1.0	1.0	1.0	1.0

**Table 3.** NC values after applying various noise attacks (without keys).

No	Attack Type	Lena	Peppers	Baboon	Fruit
1	Gaussian (0.1)	0.9997	0.9823	1.0	0.9351
2	Speckle (0.01)	0.8835	0.9292	0.9068	0.9349
3	Adjustment	0.9543	0.7544	0.9014	0.6137
4	Cropping (50%)	0.7919	0.7821	0.7912	0.7866
5	Sharpening (tol = 0.1)	0.9578	0.9335	0.9241	0.8594
6	Rotation ( $40^0$ )	0.5160	0.5132	0.5194	0.5193
7	Wiener filtering	0.6753	0.6785	0.6884	0.6771
8	Poison noise	0.9950	0.9963	0.9992	0.9990
9	Salt and pepper noise (0.01)	0.9945	0.9931	0.9956	0.9944
10	Median filtering	0.9762	0.9541	0.9896	0.9459
11	Compression (quality factor = 50%)	0.5775	0.5936	0.5912	0.5676

Table 4 shows a comparative analysis between the proposed and several recent state-of-the-art methods [13,23,24] for NC against different attacks. From this table, it is observed that the NC of the proposed method is numerically one against various attacks using keys, in contrast to state-of-the-art methods whose NC vary from 0.7991 to 0.9999. It should be mentioned that Ahmed et al. [23] shows low robustness against rotation and salt and pepper noise attack, and Su et al. [13] shows low robustness against median filtering and JPEG compression attack. In all other cases, these two methods show good robustness. Moreover, Patvardhar et al. [24] shows good robustness against various attacks.

**Table 4.** A comparative analysis between the proposed and several recent methods in terms of NC.

No	Attack Type	Ahmed et al. [23]	Patvardhar et al. [24]	Su et al. [13]	Proposed
1	Gaussian noise (0.1)	0.9625	0.9885	0.9131	1.0
2	Speckle noise (0.01)	0.9601	–	–	1.0
3	Contrast Adjustment	–	0.9491	–	1.0
4	Cropping (50%)	–	0.9947	0.9604	1.0
5	Sharpening	0.9388	–	0.9999	1.0
6	Rotation (25°)	0.7991	0.9989	–	1.0
7	Poison noise	0.9884	–	–	1.0
8	Salt and pepper noise (0.01)	0.9117	0.9807	0.9902	1.0
9	Median filtering	0.9908	0.9989	0.8814	1.0
10	JPEG compression (quality factor = 20%)	0.9784	0.9895	0.8469	1.0

In other words, this proposed algorithm with its unique key approach is much more robust than any other existing method. In addition, our method utilizes the key mapping concept with singular values of the host image. This concept improves the performance of the proposed method against severe noise attack. This approach also ensures ownership with high robustness. Furthermore, Gaussian mapping enhances the security of the watermark. Finally, coefficient ordering in the smaller block provides high imperceptibility. The concatenation of smaller blocks into the larger block provides high robustness against noise attack. In a nutshell, it can be concluded that our proposed method outperforms recent state-of-the-art methods in terms of robustness, security, and imperceptibility.

## 5. Conclusions

This paper presented an image watermarking scheme using FWHT, SVD, key mapping, and coefficient ordering. FWHT is chosen because of its low computational complexity. To enhance the robustness of the proposed method against severe attacks, key mapping is introduced using SVD. It is used because unique keys are generated from the singular values of the FWHT blocks of the cover image. Furthermore, Gaussian mapping is used to scramble the watermark. This makes the system secured against unauthorized detection. Thus, the proposed method ensures high robustness as well as high security against numerous attacks. Experimental results indicated that the proposed scheme shows better results than the recent methods in terms of robustness and security. Moreover, it yielded high-quality watermarked images. The NC value of the proposed method is numerically one, while the PSNR of it lies between 49.78 and 52.64. In contrast, the recent state-of-the-art methods show that the NC varies from 0.7991 to 0.9999, while the PSNR resides between 39.4428 and 54.2599. These results verified that the proposed method could be effectively utilized for image copyright protection and proof of ownership. We will extend the proposed method for video watermarking in the future.

**Author Contributions:** All authors contributed equally to the conception of the idea, the design of experiments, the analysis and interpretation of results, and the writing and improvement of the manuscript. All authors have read and agreed to the published version of the manuscript.

**Funding:** This work was supported by the Korea Institute of Energy Technology Evaluation and Planning (KETEP) and the Ministry of Trade, Industry and Energy (MOTIE) of the Republic of Korea (20192510102510, 20172510102130)

**Conflicts of Interest:** The authors declare no conflict of interest.

## References

1. Bakhsh, F.Y.; Moghaddam, M.E. A robust HDR images watermarking method using artificial bee colony algorithm. *J. Inf. Secur. Appl.* **2018**, *41*, 12–27.
2. Guo, Y.; Au, O.C.; Wang, R.; Fang, L.; Cao, X. Halftone image watermarking by content aware double-sided embedding error diffusion. *IEEE Trans. Image Process.* **2018**, *27*, 3387–3402. [[CrossRef](#)] [[PubMed](#)]
3. Chetan, K.R.; Nirmala, S. An efficient and secure robust watermarking scheme for document images using Integer wavelets and block coding of binary watermarks. *J. Inf. Secur. Appl.* **2015**, *24*, 13–24. [[CrossRef](#)]

4. Wanga, H.; Yina, B.; Zhou, L. Geometrically invariant image watermarking using connected objects and gravity centers. *KSII Trans. Internet Inf. Syst.* **2013**, *7*, 2893–2912.
5. Lin, P.Y.; Chen, Y.H.; Chang, C.C.; Lee, J.S. Contrast adaptive removable visible watermarking (CARVW) mechanism. *Image Vis. Comput.* **2013**, *31*, 311–321. [[CrossRef](#)]
6. Su, Q.; Niu, Y.; Zou, H.; Liu, X. A blind dual color images watermarking based on singular value decomposition. *Appl. Math. Comput.* **2013**, *219*, 8455–8466. [[CrossRef](#)]
7. Wu, X.; Sun, W. Robust copyright protection scheme for digital images using overlapping DCT and SVD. *Appl. Soft Comput.* **2013**, *13*, 1170–1182. [[CrossRef](#)]
8. Bhatnagar, G.; Wua, Q.M.J.; Raman, B. A new robust adjustable logo watermarking scheme. *Comput. Secur.* **2012**, *31*, 40–58. [[CrossRef](#)]
9. Tsai, H.H.; Huang, Y.J.; Lai, Y.S. An SVD-based image watermarking in wavelet domain using SVR and PSO. *Appl. Soft Comput.* **2012**, *12*, 2442–2453. [[CrossRef](#)]
10. Hun, H.T.; Chen, W.H. A dual cepstrum based watermarking scheme with self-synchronization. *Signal Process.* **2012**, *92*, 1109–1116.
11. Lin, C.C. An information hiding scheme with minimal image distortion. *Comput. Stand. Interfaces* **2011**, *33*, 477–484. [[CrossRef](#)]
12. Lee, Y.; Kim, H.; Park, Y. A new data hiding scheme for binary image authentication with small image distortion. *Inf. Sci.* **2009**, *179*, 3866–3884. [[CrossRef](#)]
13. Su, Q.; Wang, G.; Zhang, X. A new algorithm of blind color image watermarking based on LU decomposition. *Multidimens. Syst. Signal Process.* **2018**, *29*, 1055–1074. [[CrossRef](#)]
14. Murty, P.S.; Kumar, S.D.; Kumar, P.R. A semi blind self reference image watermarking in DCT using Singular Value Decomposition. *Int. J. Comput. Appl.* **2013**, *62*, 29–36.
15. Shen, J.J.; Ren, J.M. A robust associative watermarking technique based on vector quantization. *Digit. Signal Process.* **2010**, *20*, 1408–1423. [[CrossRef](#)]
16. Bhatnagar, G.; Raman, B. A new robust reference watermarking scheme based on DWT-SVD. *Comput. Stand. Interfaces* **2009**, *31*, 1002–1013. [[CrossRef](#)]
17. Zhou, X.; Zhang, H.; Wang, C. A robust image watermarking technique based on DWT, APDCBT, and SVD. *Symmetry* **2018**, *10*, 77. [[CrossRef](#)]
18. Sarker, M.I.H.; Khan, M.I. An efficient image watermarking scheme using BFS technique based on Hadamard Transform. *Smart Comput. Rev.* **2013**, *3*, 298–308.
19. Kumar, A.; Luhach, A.K.; Pal, D. Robust digital image watermarking technique using image normalization and Discrete Cosine Transformation. *Int. J. Comput. Appl.* **2013**, *65*, 5–13.
20. Liua, J.; Liub, G.; Hea, W.; Lia, Y. A new digital watermarking algorithm based on WBCT. *Procedia Eng.* **2012**, *29*, 1559–1564. [[CrossRef](#)]
21. Lai, C.C.; Tsai, C.C. Digital image watermarking using Discrete Wavelet Transform and Singular Value Decomposition. *IEEE Trans. Instrum. Meas.* **2010**, *59*, 3060–3063. [[CrossRef](#)]
22. Mohammad, A.A.; Alhaj, A.; Shaltaf, S. An improved SVD-based watermarking scheme for protecting rightful ownership. *Signal Process.* **2008**, *88*, 2158–2180. [[CrossRef](#)]
23. Ahmed, K.A.; Ozturk, S. A novel hybrid DCT and DWT based robust watermarking algorithm for color images. *Multimed. Tools Appl.* **2019**, *78*, 17027–17049.
24. Patvardhan, C.; Kumar, P.; Lakshmi, C.V. Effective color image watermarking scheme using YCbCr color space and QR code. *Multimed. Tools Appl.* **2018**, *77*, 12655–12677. [[CrossRef](#)]

